

Prestack depth migration by symmetric nonstationary phase shift

Robert J. Ferguson and Gary F. Margrave

ABSTRACT

A new depth imaging method is presented that is based on nonstationary filter theory. It is suitable for imaging media whose velocity structure varies in all spatial coordinates. The well-known phase-shift-plus-interpolation method and the recently introduced nonstationary phase-shift method, both implemented as nonstationary filters, are combined into a single symmetric operator. The symmetric operator is used to compute incident and reflected wavefields at different depths using, respectively, a source waveform and geophone recordings. The ratio of the resulting incident and reflected wavefields is used to estimate seismic reflectivity. Reflectivity is then immediately useful in providing a kinematic image of the subsurface. A practical implementation of the symmetric operator is possible when the required velocity model is made piecewise constant laterally. Depth imaging then proceeds by a sequence of phase shifts, spatial windows and integrations over temporal frequency. Migration of the Marmousi synthetic data set by this method provides a very good image.

INTRODUCTION

The phase-shift method (Gazdag, 1978) predicts the amplitudes and phases of wavefields at depth based on known wavefields at shallower depths and a model of the subsurface velocities. The known wavefields are usually modeled seismic source wavefields and geophone recordings, and the velocity model is usually inferred from geologic mapping, sonic logs and seismic semblance analysis. Phase-shifted wavefields are used to compute seismic reflectivity in the subsurface that can be used to estimate the acoustic velocity of rocks (assuming an analytic relationship between density and velocity) at a scale much finer than the original velocity model. Phase-shifting wavefields is a perfectly stable process and gives exact results for phase angles up to 90 degrees if the acoustic velocity of the medium is everywhere constant (Gazdag, 1978; Stoffa et al., 1990). Historically, velocity variation in depth has been accommodated by recursively phase-shifting wavefields through small depth intervals of constant velocity (Gazdag, 1978). The process occurs entirely in the Fourier domain with the usual advantages in speed and accuracy (Whitmore et al., 1988). An additional advantage of phase shift is that reflections, multiple reflections, head waves and mode conversions are not generated by velocity-model gradients to confuse the resulting images (Holberg, 1988). (This last point assumes the inferred velocity model is a smooth approximation of the true velocity, thus all propagating modes are effectively decoupled.)

Approximate phase shifts for laterally variable velocity can be done using the split-step-Fourier (Stoffa et al., 1990), and phase-screen (Wu, 1994) methods, that split the process into a focussing step and a vertical time delay. The delay is

computed in the space-temporal frequency domain and accommodates lateral velocity variations. Focussing occurs in the Fourier domain and assumes velocity is either constant (Stoffa et al., 1990), or approximately accommodates lateral velocity variations (Wu, 1994). Another method, phase-shift-plus-interpolation (PSPI; Gazdag and Sguazzero, 1984), extends phase-shift to laterally variable velocity by computing a number of constant-velocity phase shifts, for a set of reference velocities, and interpolating to obtain a single laterally variable result (Gazdag and Sguazzero, 1984).

Black et al. (1984) give an analytic expression for a Fourier method that accommodates lateral velocity variation but provide little insight into its nature. Margrave and Ferguson (1997, 1999a) show that the method of Black et al. (1984) is a generalization of PSPI to an exhaustive set of reference velocities that avoids all interpolation. Margrave and Ferguson (1997, 1999a) also use nonstationary filter theory (Margrave, 1998) to derive the adjoint form to PSPI called nonstationary phase shift (NSPS).

In this paper, we show how NSPS and PSPI can be combined into a single operator that has the virtue of being symmetric in the domain of space and temporal frequency. We then detail the structure of a practical prestack depth migration of source records. To gain computational efficiency, we approximate the actual velocity variation within a given depth step by a piecewise constant function. As an example, the Marmousi model of the Institute Francais du Petrole (IFP) (Bourgeois et al., 1991) is used. The model consists of 240 source gathers, the source impulse, velocity and density for the entire model. IFP used finite differences to generate the seismic data so elastic wave motion is approximated and some dispersion is present (Bourgeois et al., 1991).

REVIEW OF CONSTANT VELOCITY PHASE SHIFT

A review of constant-velocity phase shift (Gazdag, 1978) is helpful in understanding its nonstationary (variable-velocity) extension. The phase-shift method is most useful in situations where only macro contrasts in the required velocity model are known in depth so, reflections, multiple reflections, head waves and mode conversions cannot be modeled, and the elastic wave equation is unnecessary. Propagation is assumed governed by the scalar wave equation, and Fourier transforms are used to decompose seismic wavefields into planewaves that are phase shifted from the surface to new depths. The results are then inverse Fourier transformed into new wavefields that are used to estimate reflectivity. In the classical derivation, velocity must remain constant in all coordinates. However, if the subsurface is divided into depth intervals of differing velocities, then wavefields can be phase shifted one depth interval at a time and reflectivity estimated at each depth. The output of one phase shift becomes the input to the next and so on. Continuous velocity variation in depth is then accommodated in the limit of infinitesimally small depth intervals.

Assuming a monochromatic wavefield ψ of frequency ω and spatial coordinates $\mathbf{x}_0 = (x, y, z)$ where

$$\psi(\mathbf{x}_0, t) = \psi(\mathbf{x}_0, \omega) \exp(\pm i\omega t) \quad (1)$$

a scalar wave equation for heterogeneous media is,

$$\nabla^2 \psi(\mathbf{x}_0, \omega) = -\left(\frac{\omega}{c(\mathbf{x}_0)}\right)^2 \psi(\mathbf{x}_0, \omega) \quad (2)$$

The wavefield ψ can be represented by an inverse Fourier transform of its spectrum ϕ

$$\psi(\mathbf{x}_0, \omega) = \frac{1}{(2\pi)^3} \int \phi(\mathbf{k}_0, \omega) \exp(-i\mathbf{x}_0 \cdot \mathbf{k}_0) d\mathbf{k}_0 \quad (3)$$

where coordinates $\mathbf{k}_0 = (k_x, k_y, k_z)$ are the Fourier duals (wavenumbers) of \mathbf{x}_0 . Replace ψ in equation (2) with equation (3) and compute the partial derivatives

$$\int [\mathbf{k}_0 \cdot \mathbf{k}_0] \phi(\mathbf{k}_0, \omega) \exp(-i\mathbf{x}_0 \cdot \mathbf{k}_0) d\mathbf{k}_0 = \left(\frac{\omega}{c(\mathbf{x}_0)}\right)^2 \int \phi(\mathbf{k}_0, \omega) \exp(-i\mathbf{x}_0 \cdot \mathbf{k}_0) d\mathbf{k}_0 \quad (4)$$

Then, Fourier transform equation (4)

$$[\mathbf{k}_0 \cdot \mathbf{k}_0] \phi(\mathbf{k}_0, \omega) = \int \phi(\mathbf{k}'_0, \omega) \int \left(\frac{\omega}{c(\mathbf{x}_0)}\right)^2 \exp(-i\mathbf{x}_0 \cdot [\mathbf{k}'_0 - \mathbf{k}_0]) d\mathbf{x}_0 d\mathbf{k}'_0 \quad (5)$$

where the order of integration has been reversed. Variation of c with \mathbf{x}_0 complicates evaluation of the right hand side of equation (5). However, a general result is obtained if we constrain c to be constant. Thus, for a homogeneous medium $c(\mathbf{x}_0) = c$, equation (5) reduces to

$$[\mathbf{k}_0 \cdot \mathbf{k}_0] \phi(\mathbf{k}_0, \omega) = \left(\frac{\omega}{c}\right)^2 \int \phi(\mathbf{k}'_0, \omega) \delta(\mathbf{k}'_0 - \mathbf{k}_0) d\mathbf{k}'_0 \quad (6)$$

or,

$$[\mathbf{k}_0 \cdot \mathbf{k}_0] = \left(\frac{\omega}{c}\right)^2 \quad (7)$$

Equation (7) is known as the dispersion relation for scalar waves, that allows k_z to be computed from quantities which can be measured at $z = 0$; that is k_x , k_y and ω ,

$$\left[k_z^2 + \mathbf{k} \cdot \mathbf{k} \right] = \left(\frac{\omega}{c} \right)^2 \Rightarrow k_z = \pm \sqrt{\left(\frac{\omega}{c} \right)^2 - \mathbf{k} \cdot \mathbf{k}}, \quad (8)$$

where $\mathbf{k} = \{k_x, k_y\}$. Spectrum φ in equation (3) can be modified to force the k_z dependence of equation (8)

$$\varphi(\mathbf{k}, k_z, \omega) = \varphi_1(\mathbf{k}, \omega) \delta \left(k_z + \sqrt{\left(\frac{\omega}{c} \right)^2 - \mathbf{k} \cdot \mathbf{k}} \right) + \varphi_2(\mathbf{k}, \omega) \delta \left(k_z - \sqrt{\left(\frac{\omega}{c} \right)^2 - \mathbf{k} \cdot \mathbf{k}} \right) \quad (9)$$

where φ_1 and φ_2 are arbitrary functions of (\mathbf{k}, ω) to be determined from boundary conditions. The k_z dependence is contained entirely by delta functions, whose action in equation (3) is to replace k_z everywhere and collapse the k_z integral thus,

$$\psi(\mathbf{x}, z, \omega) = \frac{1}{(2\pi)^2} \int [\varphi_1(\mathbf{k}, \omega) \alpha(\mathbf{k}, z, \omega) + \varphi_2(\mathbf{k}, \omega) \alpha(\mathbf{k}, -z, \omega)] \exp(-i\mathbf{x} \cdot \mathbf{k}) d\mathbf{k} \quad (10)$$

where

$$\alpha(\mathbf{k}, \pm z, \omega) = \exp \left(\pm iz \sqrt{\left(\frac{\omega}{c} \right)^2 - \mathbf{k} \cdot \mathbf{k}} \right) \quad (11)$$

is the phase-shift extrapolator. We adopt the convention that z increases downward. Equation (10) defines ψ for all z and separates it into up travelling (φ_1) and down travelling (φ_2) components as can be seen in the sign dependence on z . In the absence of vertical-velocity gradients, but for arbitrary lateral gradients, φ_1 and φ_2 propagate independently of each other (Fishman and McCoy, 1985). Evaluation of equation (10) at $z = 0$ gives $\varphi_1 + \varphi_2$ as the spectrum of ψ recorded at the surface $z = 0$

$$\psi(\mathbf{x}, 0) = \frac{1}{(2\pi)^2} \int [\varphi_1(\mathbf{k}) + \varphi_2(\mathbf{k})] \exp(-i\mathbf{x} \cdot \mathbf{k}) d\mathbf{k} \quad (12)$$

(the dependence on ω has been suppressed). The complete determination of both φ_1 and φ_2 requires the first derivative of ψ with respect to depth evaluated at $z = 0$ as a second boundary condition. Since the derivative is generally not available, we make the common assumption that only waves travelling upwards are recorded. Then, only $\varphi_1 = \varphi$ is nonzero and equation (10) reduces to

$$\psi(\mathbf{x}, z) = \frac{1}{(2\pi)^2} \int \varphi(\mathbf{k}, 0) \alpha(\mathbf{k}, z) \exp(-i\mathbf{x} \cdot \mathbf{k}) d\mathbf{k} \quad (13)$$

Equation (13) allows $\psi(z = 0)$ to be phase shifted to any depth z .

NONSTATIONARY PHASE SHIFT

Wavefields phase shifted in constant velocity media are exact solutions to the scalar wave equation. For laterally variable velocity, three alternative approximations are developed here using nonstationary filter concepts (Margrave, 1998). One is proposed by Margrave and Ferguson (1999a) and is referred to as nonstationary phase shift (NSPS). Margrave and Ferguson (1999a) recognize the other as the phase-shift-plus-interpolation method (PSPI; Gazdag and Sguazzero, 1984) applied in the limit of continuous velocity variation. (The continuous form of PSPI contains no interpolation.) A third method that we derive here combines NSPS and PSPI into a single operator that has the desirable property of being symmetric in the (\mathbf{x}, ω) domain. NSPS and PSPI also correspond to, respectively, the standard and adjoint standard forms of pseudo-differential operators whose symbols are the nonstationary phase-shift extrapolator α .

A direct way to accommodate laterally variable velocity in equation (13) is to simply allow α to have \mathbf{x} dependence through $c(\mathbf{x})$. That is,

$$\psi(\mathbf{x}, z) = \frac{1}{(2\pi)^2} \int \varphi(\mathbf{k}, 0) \alpha(\mathbf{x}, \mathbf{k}, z) \exp(-i\mathbf{x} \cdot \mathbf{k}) d\mathbf{k} \quad (14)$$

where the nonstationary extrapolator is

$$\alpha(\mathbf{x}, \mathbf{k}, z, \omega) = \exp \left(iz \sqrt{\left(\frac{\omega}{c(\mathbf{x})} \right)^2 - \mathbf{k} \cdot \mathbf{k}} \right). \quad (15)$$

In this expression \mathbf{x} corresponds to *output* coordinates, at z , so velocity varies with output location. Equation (14) applies a nonstationary phase shift carrying the spectrum $\varphi(z = 0)$ to a new depth simultaneous with transformation to space coordinates. Fishman and McCoy (1985) suggest the same simple extension to constant-velocity phase-shift for large ω , but do not recognize PSPI in the limit of continuously variable velocity (see Margrave and Ferguson, 1999a, for a justification).

Equation (14) can be written to explicitly contain the input wavefield by replacing $\varphi(z = 0)$ with the Fourier transform of $\psi(z = 0)$

$$\psi(\mathbf{x}, z) = \int \psi(\mathbf{y}, 0) A(\mathbf{x}, \mathbf{y}, z) d\mathbf{y} \quad (16)$$

where,

$$A(\mathbf{x}, \mathbf{y}, z) = \frac{1}{(2\pi)^2} \int \alpha(\mathbf{x}, \mathbf{k}, z) \exp(i[\mathbf{y} - \mathbf{x}] \cdot \mathbf{k}) d\mathbf{k} \quad (17)$$

and \mathbf{y} corresponds to the lateral coordinates (*input* coordinates) at $z = 0$. Equation (14) is a standard-form pseudo differential operator where $\alpha(\mathbf{x}, \mathbf{y}, z)$ is the symbol of the

operator. Equation (16) presents the same operator as a singular integral (Stein, 1993: 230 – 233).

An alternative variable-velocity phase shift follows by returning to the constant velocity case (equation (13)) and Fourier transforming

$$\varphi(\mathbf{k}, z) = \varphi(\mathbf{k}, 0)\alpha(\mathbf{k}, z) \quad (18)$$

Next, replace $\varphi(z = 0)$ with the Fourier transform of $\psi(z = 0)$

$$\varphi(\mathbf{k}, z) = \int \psi(\mathbf{y}, 0)\exp(i\mathbf{y} \cdot \mathbf{k})d\mathbf{y}\alpha(\mathbf{k}, z) \quad (19)$$

Since velocity is independent of position, α can be moved inside the Fourier integral

$$\varphi(\mathbf{k}, z) = \int \psi(\mathbf{y}, 0)\alpha(\mathbf{k}, z)\exp(i\mathbf{y} \cdot \mathbf{k})d\mathbf{y} \quad (20)$$

Velocity is now allowed to vary with input coordinate \mathbf{y}

$$\varphi(\mathbf{k}, z) = \int \psi(\mathbf{y}, 0)\alpha(\mathbf{y}, \mathbf{k}, z)\exp(i\mathbf{y} \cdot \mathbf{k})d\mathbf{y} \quad (21)$$

Equation (21) is a nonstationary phase shift carrying wavefield $\psi(z = 0)$ to a new depth simultaneous with a transformation to wavenumbers. Margrave and Ferguson (1997, 1999a) describe this form for seismic imaging calling it nonstationary phase shift (NSPS). Next, inverse Fourier transform equation (21)

$$\psi(\mathbf{x}, z) = \int \psi(\mathbf{y}, 0)B(\mathbf{x}, \mathbf{y}, z)d\mathbf{y} \quad (22)$$

where,

$$B(\mathbf{x}, \mathbf{y}, z) = \frac{1}{(2\pi)^2} \int \alpha(\mathbf{y}, \mathbf{k}, z)\exp(i[\mathbf{y} - \mathbf{x}] \cdot \mathbf{k})d\mathbf{k} \quad (23)$$

We recognize equation (22) as the adjoint of a pseudo differential operator whose symbol is α^* . To demonstrate we simply show that the adjoint of $B(\mathbf{x}, \mathbf{y}, z)$ is $A(\mathbf{x}, \mathbf{y}, -z)$. That is

$$\begin{aligned} B(\mathbf{y}, \mathbf{x}, z) &= \frac{1}{(2\pi)^2} \int \alpha(\mathbf{y}, \mathbf{k}, -z)\exp(-i[\mathbf{y} - \mathbf{x}] \cdot \mathbf{k})d\mathbf{k} \\ &= \frac{1}{(2\pi)^2} \int \alpha(\mathbf{x}, \mathbf{k}, -z)\exp(i[\mathbf{y} - \mathbf{x}] \cdot \mathbf{k})d\mathbf{k} \\ &= A(\mathbf{x}, \mathbf{y}, -z) \end{aligned} \quad (24)$$

where superscript \dagger represents the adjoint (Hermitian conjugate). (Velocity variation at \mathbf{x} and \mathbf{y} must be the same for equation (24) to hold.) Thus, the adjoint of the NSPS

operator B is the PSPI operator A with the depth value z changed in sign. Similarly, the adjoint of PSPI is NSPS propagating in the opposite direction.

A NEW SYMMETRIC NONSTATIONARY PHASE SHIFT

The complimentary relationship between NSPS and PSPI suggests that it is natural to combine them into a third, variable-velocity phase shift that may perform better than PSPI or NSPS alone. Etgen (1994) demonstrates that operators like PSPI can become unstable in the presence of instantaneous velocity contrasts of thousands of meters-per-second. Margrave and Ferguson (1999b), expanding on the work of Etgen (1994), demonstrate that the NSPS operator also suffers from instability, but that a hybrid of the two, dubbed symmetric nonstationary phase shift (SNPS), has greater stability. We will show that the SNPS operator has the spatial symmetry required by reciprocity (Wapenaar and Grimbergen, 1998).

The symmetric operator (i.e., its kernel equals its transpose) results by phase shifting from 0 to $z/2$ by NSPS and from $z/2$ to z by PSPI or vice versa. (Note: PSPI followed by NSPS is symmetric but does not result in an identical extrapolator.) For example, using equation (21), phase shift $\psi(z=0)$ from 0 to $z/2$ by NSPS

$$\phi(\mathbf{k}, z/2) = \int \psi(\mathbf{y}, 0) \alpha(\mathbf{y}, \mathbf{k}, z/2) \exp(i\mathbf{y} \cdot \mathbf{k}) d\mathbf{y} \quad (25)$$

Next, using equation (14), phase shift from $z/2$ to z by PSPI

$$\psi(\mathbf{x}, z) = \frac{1}{(2\pi)^2} \int \phi(\mathbf{k}, z/2) \alpha(\mathbf{x}, \mathbf{k}, z/2) \exp(-i\mathbf{x} \cdot \mathbf{k}) d\mathbf{k} \quad (26)$$

Replace ϕ in equation (26) by equation (25) and switch the order of integration to give

$$\psi(\mathbf{x}, z) = \int \psi(\mathbf{y}, 0) C(\mathbf{x}, \mathbf{y}, z) d\mathbf{y} \quad (27)$$

where C , the kernel of the SNPS operator, is defined as

$$C(\mathbf{x}, \mathbf{y}, z) = \frac{1}{(2\pi)^2} \int \alpha(\mathbf{y}, \mathbf{k}, z/2) \alpha(\mathbf{x}, \mathbf{k}, z/2) \exp(-i\mathbf{k} \cdot [\mathbf{x} - \mathbf{y}]) d\mathbf{k} \quad (28)$$

Equation (27) is an (\mathbf{x}, ω) form of a nonstationary phase shift that combines NSPS and PSPI in a single, symmetric operator C (equation (27)). The symmetry of C is evident by its invariance under the exchange of coordinates \mathbf{y} and \mathbf{x} . The SNPS extrapolator is an explicit extrapolator suitable for 2D or 3D depth migration in complex media. Wapenaar and Grimbergen (1998) use reciprocity concepts to argue that such extrapolators should be symmetric in the (\mathbf{x}, ω) domain. We note that ordinary phase shift has such symmetry and has the property that the adjoint operation simply reverses the extrapolation. SNPS has these same properties.

SYMMETRIC NONSTATIONARY PHASE SHIFT OF SOURCES AND RECEIVERS FOR DEPTH IMAGING

At a particular depth the ratio of the source (incident) seismic wavefield ψ_S , and the reflected seismic wavefield ψ_R , defines seismic reflectivity r that can be related to rock properties (e.g. P-wave velocity, S-wave velocity, density), and group angle. By recursively phase shifting the reference wavefields, $\psi_S(z = 0)$ and $\psi_R(z = 0)$, to depths $z = (0, z_1, z_2, \dots, z_n)$ r is estimated for all coordinates relevant to the recording aperture. By recursion, we mean a process like the following: 1) $\psi_S(z = 0)$ and $\psi_R(z = 0)$ are phase-shifted to $\psi_S(z_1)$ and $\psi_R(z_1)$ respectively, and $r(z_1)$ is computed; 2) $\psi_S(z_1)$ and $\psi_R(z_1)$ are phase-shifted to $\psi_S(z_2)$ and $\psi_R(z_2)$ respectively, $r(z_2)$ is computed; and 3) the process continues until r for the final depth level z_n is computed.

For any depth, ψ_R and ψ_S are not directly measurable but can be deduced from a surface recording $\psi_R(z = 0)$, and a model of the source $\psi_S(z = 0)$. For example, phase shifting $\psi_R(z = 0)$ to a new depth z is achieved with SNPS (equation (27))

$$\psi_R(\mathbf{x}, z, t) = \iint \psi_R(\mathbf{y}, 0, \omega) C(\mathbf{x}, \mathbf{y}, z, \omega) d\mathbf{y} \exp(i\omega t) d\omega, \quad (29)$$

where ω is here explicitly stated. Phase shifting $\psi_S(z = 0)$ is similarly described by,

$$\psi_S(\mathbf{x}, z, t) = \iint \psi_S(\mathbf{y}, 0, \omega) C(\mathbf{x}, \mathbf{y}, -z, \omega) d\mathbf{y} \exp(i\omega t) d\omega. \quad (30)$$

The sign reversal on z in C is required to extrapolate downward-travelling waves down while equation (29) moves upward-travelling waves down. Amplitudes characteristic of geometric spreading are contained in ψ_R and ψ_S , and amplitude variations characteristic of material contrasts are only found in ψ_R . Their ratio defines reflectivity r at depth z

$$r(\mathbf{x}, z) = \frac{\psi_R(\mathbf{x}, z, t = \tau(\mathbf{x}, z))}{\psi_S(\mathbf{x}, z, t = \tau(\mathbf{x}, z))} \quad (31)$$

where time τ is the instant ψ_S is converted into ψ_R (Temme, 1984). The required amplitudes of ψ_R and ψ_S at $t = \tau$ must be picked (Temme, 1984; Berryhill, 1979, 1984).

An implementation of equation (31) that avoids picking reflections is to replace ψ_R and ψ_S with their inverse Fourier transforms

$$r(\mathbf{x}, z) = \frac{\int_{-\infty}^{\infty} \psi_R(\mathbf{x}, z, \omega) \exp(i\omega\tau(\mathbf{x}, z)) d\omega}{\int_{-\infty}^{\infty} \psi_S(\mathbf{x}, z, \omega) \exp(i\omega\tau(\mathbf{x}, z)) d\omega}, \quad (32)$$

then for r independent of ω

$$\int_{-\infty}^{\infty} [\Psi_R(\mathbf{x}, z, \omega) - r(\mathbf{x}, z) \Psi_S(\mathbf{x}, z, \omega)] \exp(i\omega\tau(\mathbf{x}, z)) d\omega = 0 \quad (33)$$

Equation (33) is satisfied if

$$r(\mathbf{x}, z) = \frac{\Psi(\mathbf{x}, z, \omega)_R}{\Psi(\mathbf{x}, z, \omega)_S} \quad (34)$$

Equation (34) corresponds to a single temporal frequency or *monochromatic* estimate of reflectivity. Averaging r over the range of available ω gives

$$\begin{aligned} \tilde{r}(\mathbf{x}, z) &= \frac{1}{[\omega_{\max} - \omega_{\min}]} \left[\int_{-\omega_{\max}}^{-\omega_{\min}} \frac{\Psi_R(\mathbf{x}, z, \omega)}{\Psi_S(\mathbf{x}, z, \omega)} d\omega + \int_{\omega_{\min}}^{\omega_{\max}} \frac{\Psi_R(\mathbf{x}, z, \omega)}{\Psi_S(\mathbf{x}, z, \omega)} d\omega \right] \\ &= \frac{1}{[\omega_{\max} - \omega_{\min}]} \int_{\omega_{\min}}^{\omega_{\max}} \left\{ \frac{\Psi_R^*(\mathbf{x}, z, \omega)}{\Psi_S^*(\mathbf{x}, z, \omega)} + \frac{\Psi_R(\mathbf{x}, z, \omega)}{\Psi_S(\mathbf{x}, z, \omega)} \right\} d\omega \end{aligned}$$

where * is complex conjugation. Equation (35) is suitable for estimating r in variable velocity media using a recursion in depth. Overlapping each source-receiver geometry and summing provides an image of the subsurface.

PRACTICAL IMPLEMENTATION

If lateral velocity variation is smooth, depth imaging algorithms based on NSPS, PSPI and SNPS can be optimized to reduce run time by limiting the wavenumber bandwidth of the operators (Margrave and Ferguson, 1999a). Alternatively, if lateral variation in velocity is blocky, then a piecewise constant approximation for the three methods can be obtained using windowing operations and multiple constant-velocity phase shifts (Margrave and Ferguson, 1999a). We use the latter approach here. Though we present a 2D implementation, the method extends easily to 3D.

For each unique velocity v_j along coordinate x , a window Ω_j is constructed such that it takes on a value of 1 at every x location where $c(\mathbf{x})$ takes on the value v_j and is zero otherwise. After some analysis (Margrave and Ferguson, 1999a), equation (14) (PSPI) becomes

$$\Psi(x, z, \omega) = \frac{1}{2\pi} \sum_j \Omega_j \int_{-\infty}^{\infty} \alpha_j(k_x, z, \omega) \phi(k_x, 0, \omega) \exp(-ik_x x) dx \quad (36)$$

and equation (21) (NSPS) is

$$\varphi(k_x, z, \omega) = \sum_j \alpha_j(k_x, z, \omega) \int_{-\infty}^{\infty} \Psi(x, 0, \omega) \Omega_j \exp(ik_x x) dx \quad (37)$$

where the window Ω_j is

$$\Omega_j(x) = \begin{cases} 1, & v(x) = v_j \\ 0, & \text{otherwise} \end{cases} \quad (38)$$

and

$$\alpha_j(k_x, z, \omega) = \exp\left(iz \sqrt{\left(\frac{\omega}{v_j}\right)^2 - k_x^2}\right). \quad (39)$$

Unlike equations (14) and (21), the integrations in equations (36) and (37) are all Fourier transforms. Equation (36) constructs the PSPI space-domain wavefield by using ordinary phase-shift to extrapolate the input spectrum for each of the $\{v_j\}$. Then the windows $\{\Omega_j\}$ are applied to these extrapolations and the resulting wavefields are superimposed. In contrast, equation (37) constructs the NSPS Fourier-domain wavefield by applying the window set $\{\Omega_j\}$ to the input wavefield, phase shifting each result with the appropriate v_j , and summing over all j . The essential difference is that windowing is the last step in PSPI and the first step in NSPS. The cost of NSPS or PSPI is proportional to the number of distinct velocities times the cost of ordinary phase shift.

Similarly, the SNPS operator has a piecewise-constant approximation that is the cascade of the NSPS and PSPI processes. Figures 1a, b, and Figure 2 present a set of flow charts that illustrate the implementation of, respectively, NSPS, PSPI and SNPS. These expressions accomplish nonstationary phase shift by the fast and relatively simple operations of constant-velocity phase shift and windowing.

MARMOUSI

We use the Marmousi model of the Institut Francais du Petrole (IFP) (Bourgeois et al., 1991) to demonstrate prestack imaging by nonstationary phase shift. The 2D model consists of 240 source gathers (pressure recordings), a known source impulse, plus complete velocity and density profiles. IFP used finite differences to generate the seismic data so elastic wave motion is approximated and some dispersion is present (Bourgeois et al., 1991). The underlying geological model represents a profile through the North Quenguela trough in the Cuanza basin of Angola.

We did not preprocess the Marmousi data so the embedded source wavelet and multiples are present. No attempt was made to deal with multiples, but the source waveform was used to construct the reference source wavefield during imaging. The velocity model was resampled from a four-meter sample spacing in x and z to 25 meters in x , the depth interval remains at four meters. A piecewise constant

approximation to the velocity model was made by rounding each velocity to the nearest 100 m/s, resulting in approximately 10 to 20 unique velocities laterally in each depth step. No attempt was made to determine the optimal set of constant velocities.

Depth migration one source gather proceeds as follows:

- 1) Specify the reflected wavefield as the recorded source gather, and pad it from 96 to 256 traces using zero amplitude traces (e.g., an example is given in Figure 3).
- 2) Specify the incident wavefield as the source waveform provided. Place the source waveform in a position corresponding to the source location within a gather of 256 zero amplitude traces.
- 3) Depth image with SNPS using the piecewise constant velocity model. Restrict temporal frequencies to between 5 and 48 Hz.

Due to the limited recording aperture of a single source gather and the complexity of the model, a coherent image of the entire model is not possible from a single source. Figure 3 shows a source gather from location 5725m in the model. The resulting imaged gather is shown in Figure 4. Coherent reflections are only apparent in a narrow region corresponding to specular reflections, energy outside this region is noise. A complete image of the entire model is possible by migrating all of the source records, sorting the traces into common depth points (CDPs), muting noise and stacking. Figure 5 shows one CDP from location 6500 m in the model. Reflection energy on a CDP gather forms a continuous zone of coherency, as indicated by the annotated lines, data outside of this region is rejected. The resulting stacked traces (Figure 6) give reflectivity in depth but, due to stacking, they represent an average reflectivity over the range of source-receiver offsets in each CDP. For comparison, a bandlimited, zero-offset reflectivity section was computed from the p-wave velocities and densities (Figure 7).

All of the major seismic markers are present in the migrated image including three normal growth faults and the target sands. The top and bottom of the sands are resolved but the internal bedding is possibly beyond the resolution of the data. Elsewhere many of the steeply dipping folds have been imaged.

CONCLUSIONS

A commonly used phase-shift method that approximates wave motion through media with lateral variation in velocity (PSPI) is a nonstationary filter in the limit of continuous lateral velocity variation. An alternative to PSPI, nonstationary phase shift (NSPS), exists by similar intuition and nonstationary filter theory. PSPI and NSPS were shown to be, respectively, the standard and adjoint standard forms of pseudo differential operators, whose symbols are the nonstationary phase-shift extrapolator.

The PSPI and NSPS phase-shift extrapolators can be coupled to obtain a composite extrapolator, called SNPS, which is symmetric in the (x,ω) domain.

Symmetry is a desirable property (from reciprocity considerations) and is more stable. Prestack depth migration of common-source gathers was implemented using the SNPS extrapolator. Reflectivity estimates for each depth were formulated as the ratio of downward extrapolated receiver and source wavefields. This ratio was done independently for each temporal frequency and averaged over all frequencies. A practical implementation of the NSPS, PSPI and SNPS extrapolators can be done under the assumption that velocity is piecewise constant. In this case, the extrapolations are all constructed from the basic operators of constant velocity phase shift for each relevant velocity and appropriate spatial windowing. This implementation extends easily to 3D.

The Marmousi synthetic data set was used to demonstrate the viability of these results. Using a piecewise constant approximation to the exact Marmousi velocities, a very high resolution image was obtained.

ACKNOWLEDGEMENTS

We wish to thank the sponsors of CREWES for their support of this research.

REFERENCES

- Aki, K., and Richards, P. G., 1980, Quantitative seismology V1, W.H. Freeman and Company.
- Bourgeois, A., Bourget, M., Lailly, P., Poulet, M., Ricarte, P., and Versteeg, R., 1990, Marmousi, model and data: in *The Marmousi experience*, EAGE, 5 - 9.
- Berkhout, A. J., Cox, H., Verschuur, D., J., and Wapenaar, C., P., A., 1991, The Delphi approach to macro model estimation: in *The Marmousi experience*, EAGE, 87 - 111.
- Berryhill, J. R., 1979, Wave-equation datuming: *Geophysics*, **44**, 1329 - 1334.
- 1984, Wave-equation datuming before stack: *Geophysics*, **49**, 2064 - 2066.
- Etgen, J. J., 1994, Stability of explicit depth extrapolation through laterally-varying media: 64th Annual Internat. Mtg., Soc. Expl. Geophys., Expanded Abstracts, 1266-1269.
- Gazdag, J., 1978, Wave equation migration with the phase shift method: *Geophysics*, **43**, 1342 - 1351.
- Gazdag, J., and Squazero, P., 1984, Migration of seismic data by phase shift plus interpolation: *Geophysics*, **49**, 124 - 131.
- Margrave, G.F., 1998, Theory of nonstationary linear filtering in the Fourier domain with application to time-variant filtering *Geophysics*, **63**, 244 - 259.
- Margrave, G. F., and Ferguson, R. J., 1997, Wavefield extrapolation by nonstationary phase shift: 67th Annual Internat. Mtg., Soc. Expl. Geophys., Expanded Abstracts, 1599-1602.
- 1999a, Wavefield extrapolation by nonstationary phase shift: *Geophysics*, **64**, 1067-1078.
- 1999b, An explicit symmetric wavefield extrapolator for depth migration: 69th Annual Internat. Mtg., Soc. Expl. Geophys., Expanded Abstracts, (*page numbers to be determined*).
- Stein, E. M., 1993, Harmonic analysis: real-variable methods, orthogonality, and oscillatory integrals: Princeton University Press.
- Stoffa, P. L., Fokkema, J. T., de Luna Freire, R. M., and Kessinger, W. P., 1990, Split-step Fourier migration: *Geophysics*, **55**, 410-421.
- Temme, P., 1984, A comparison of common-midpoint, single-shot, and plane-wave depth migration: *Geophysics*, **49**, 1896 - 1907.
- Wapenaar, C. P. A., and Grimbergen, J.L.T., 1998, A discussion on stability analysis of wavefield depth extrapolation: Expanded abstracts 68th SEG International Convention, 1716-1719.
- Whitmore, N. D., Gray, S. H., and Gersztenkorn, A., 1988, Two-dimensional post-stack depth migration: as survey of methods, *First Break*, **6**, 189 - 197.
- Wu, R. S., 1994, Wide-angle elastic wave one-way propagation in heterogeneous media and an elastic wave complex-screen method: *J. Geophys. Res.*, **99**, 751-766.

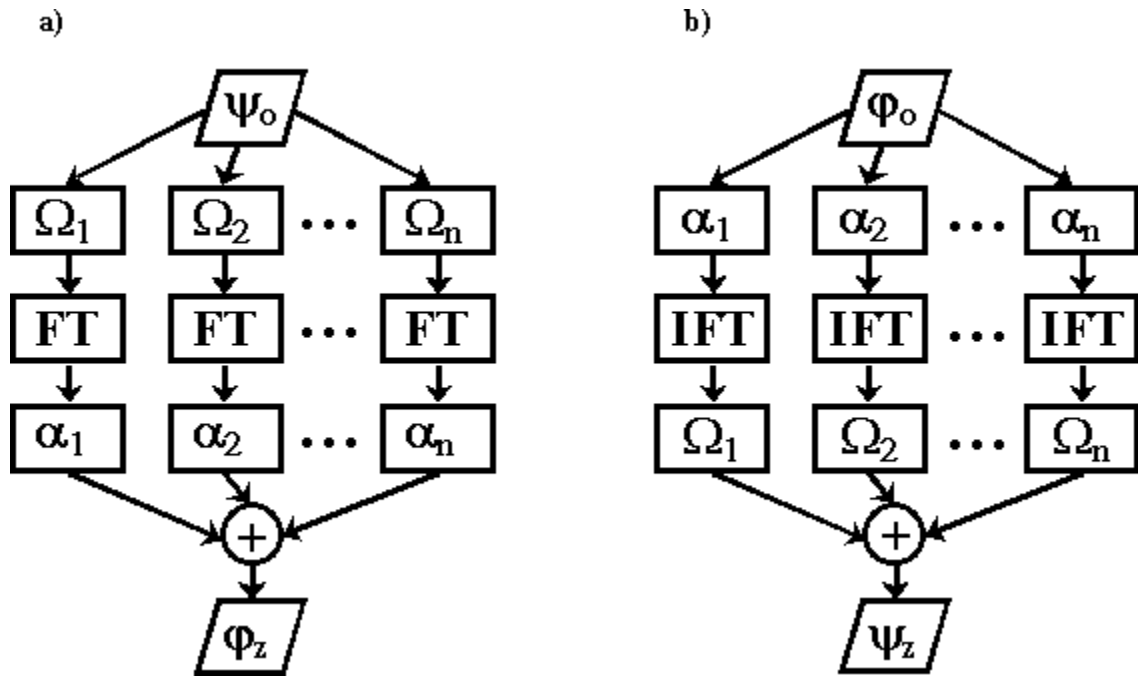


Fig. 1. Flow charts of wavefield extrapolation by NSPS (a) and PSPI (b). The windows Ω_j and phase shifts α_j correspond to piecewise constant velocities v_j . NSPS applies Ω_j to wavefield Ψ_0 prior to Fourier transforming (FT) and phase shifting. The resulting spectra are summed to form the output spectrum Φ_z . PSPI applies Ω_j to Φ_0 after phase shifting and inverse Fourier transforming (IFT). The resulting wavefields are summed to form the output wavefield Ψ_z . Both processes change spatial domain simultaneous with phase shifting, NSPS goes from x to k_x , while PSPI goes from k_x to x .

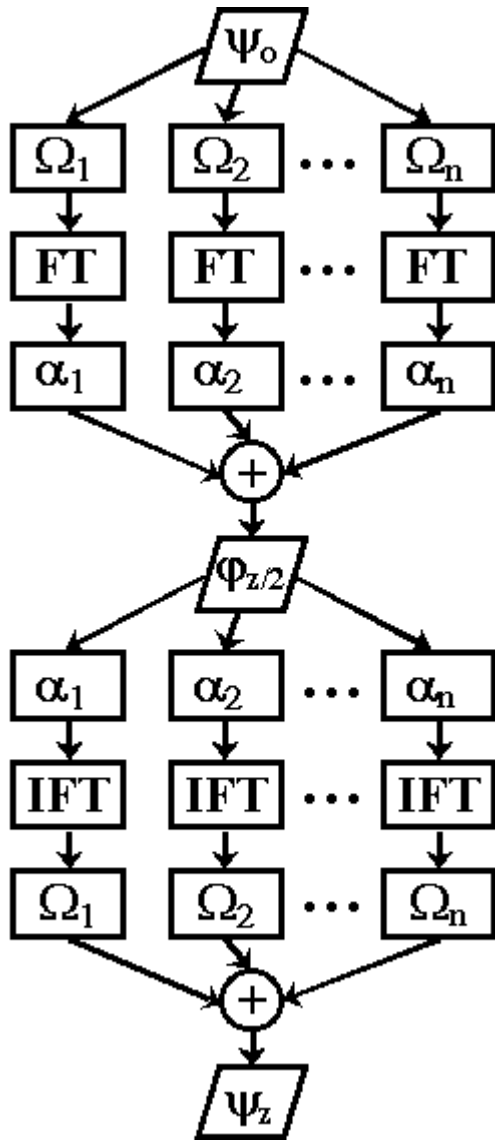


Fig. 2. Flow chart of wavefield extrapolation by SNPS. Windows Ω_j and phase shifts α_j correspond to piecewise constant velocities v_j . Phase shift of wavefield Ψ_0 to Ψ_z proceeds with a $z/2$ step by NSPS (see description in Figure 1 left) followed by a $z/2$ step by PSPI (see description in Figure 1 right). SNPS can just as easily be formulated beginning with PSPI and ending with NSPS at the cost of two extra IFTs over k_x .

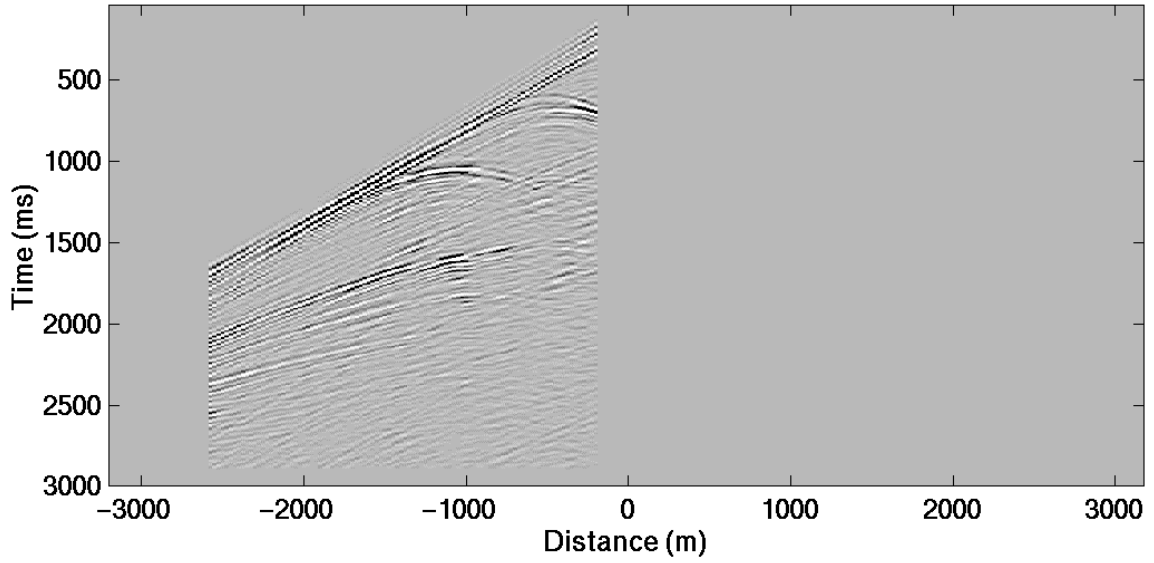


Fig. 3. A gather of common-source traces (source gather). The position of the source is at 5475 meters within the model.

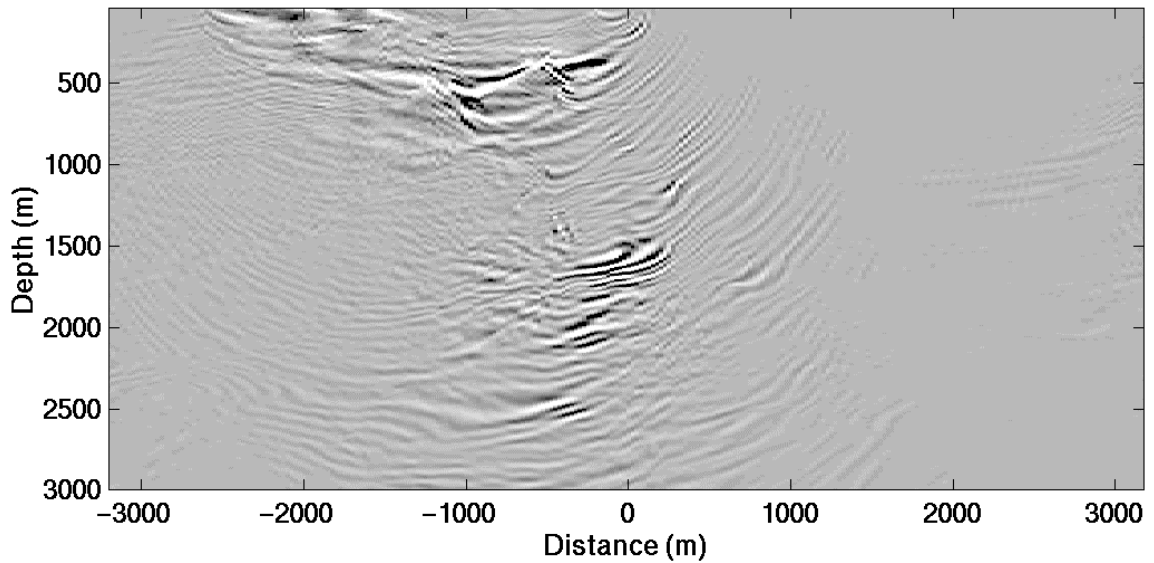


Fig. 4. Migrated image of the source gather of Figure 3. Coherent reflectivity corresponds to a narrow range of specular reflections due to the limited recording aperture (Figure 3). It is desirable to construct a complete image using a large number of overlapping images (Figure 6).

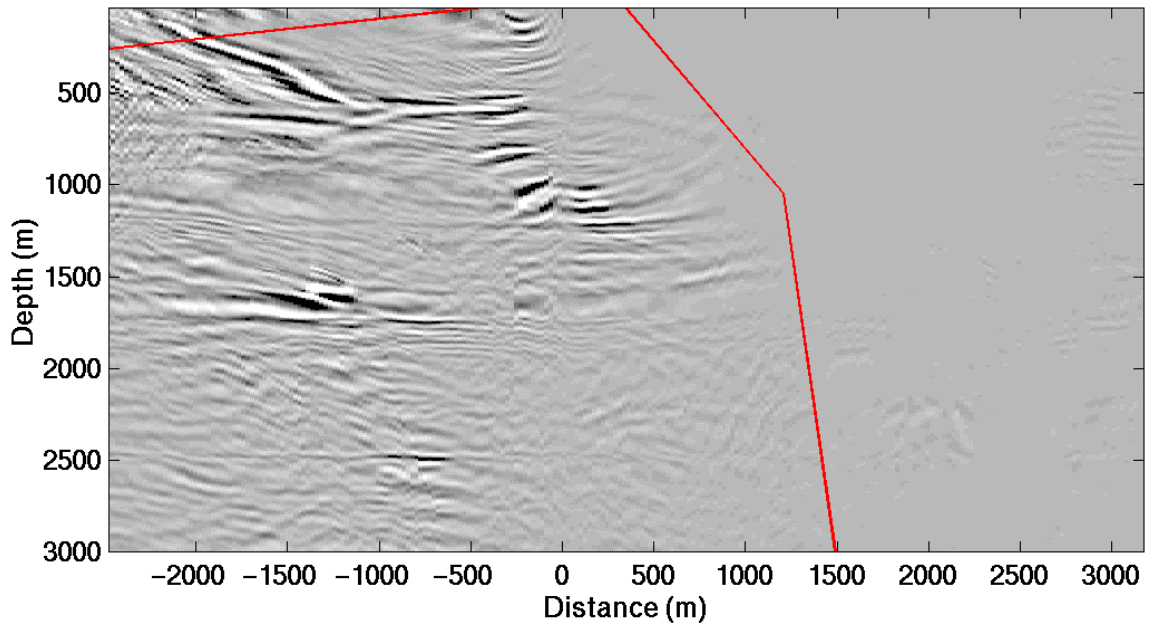


Fig. 5. A common-depth-point (CDP) gather corresponding to location 6500 m in Figure 6. Amplitudes between the mute lines (annotated) are summed to give a single trace.

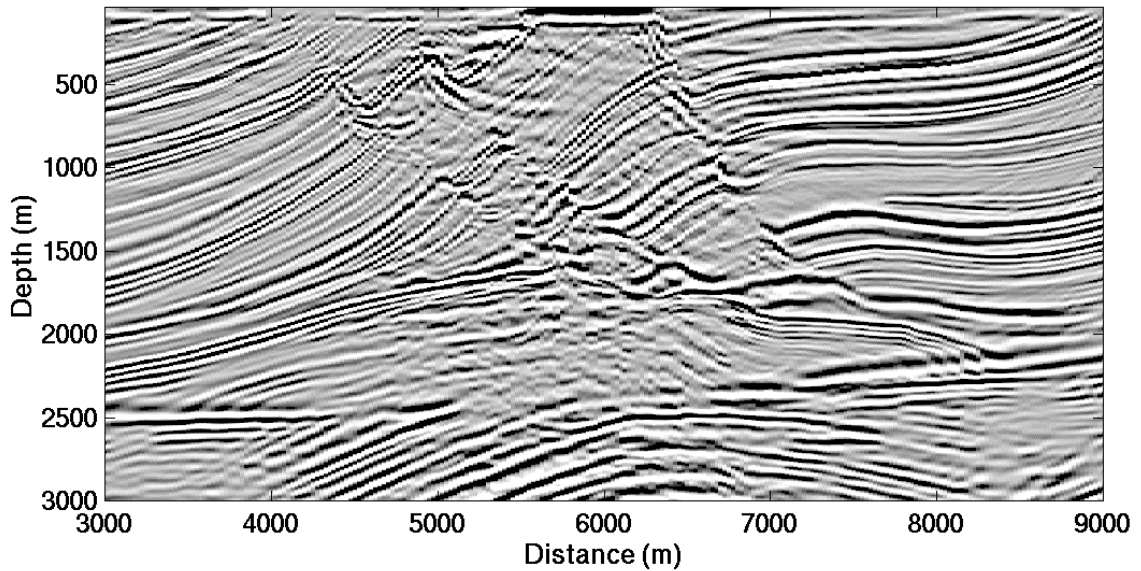


Fig. 6. Depth image from nonstationary migration. (The CDP gather in Figure 5 is muted, and summed to give the trace at distance 6500 m.) Each amplitude represents a mixed reflectivity due to stacking the CDPS. Kinematically, this figure compares favorably with the zero offset reflectivity computed from velocity and density in Figure 7. Three faults are indicated towards the top of the section with arrows. The target sand is similarly indicated towards the bottom of the section.

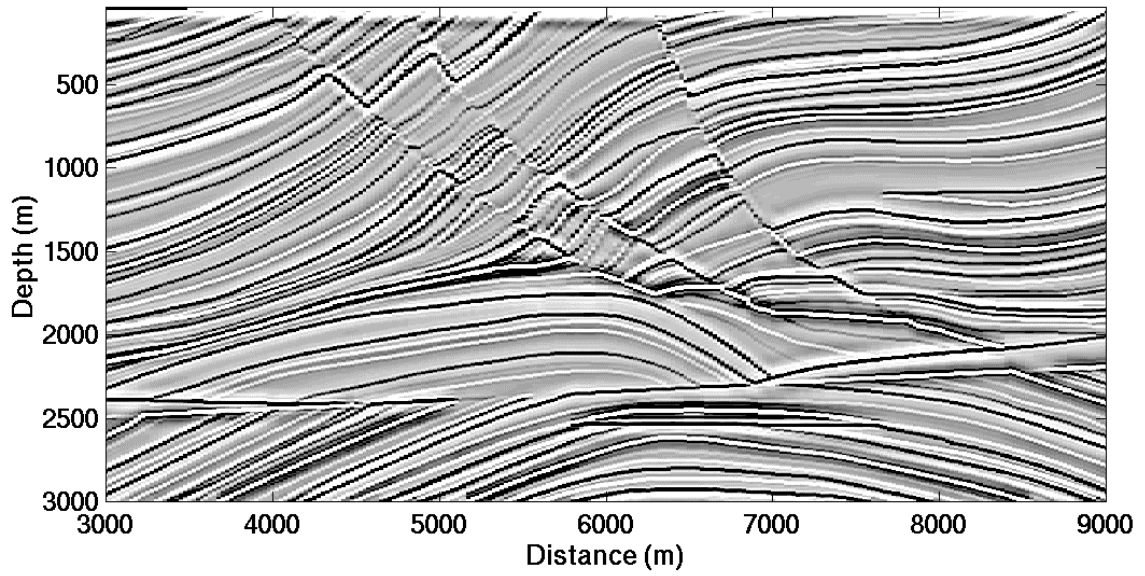


Fig. 7. Reflectivity computed from the model velocity and density. The amplitude of each point represents zero offset reflectivity. The same three faults are indicated here, as in Figure 7, towards the top of the section with arrows. The target sand is similarly indicated towards the bottom of the section.